

HOSTED BY



Egyptian Petroleum Research Institute
Egyptian Journal of Petroleum

www.elsevier.com/locate/egyjp
www.sciencedirect.com



FULL LENGTH ARTICLE

Petrophysical study of Szolnok Formation, Endrod gas field, Hungary

Abdel Muktader A. El Sayed^a, Hesham Abuseda^{b,*}, Nahla A. El Sayed^{b,1}

^a Geophysics Department, Ain Shams University, Faculty of Science, Cairo, Egypt

^b Production Department, Egyptian Petroleum Research Institute (EPRI), Cairo, Egypt

Received 2 December 2015; revised 27 February 2016; accepted 10 March 2016

KEYWORDS

Szolnok Formation;
 Great Hungarian plain;
 Petrophysical models

Abstract Results of both porosity and permeability can be used by geologists, petrophysicists, and petroleum engineers to evaluate reservoir rock, heterogeneity, and pore space history through the time of deposition and lithification. On the other hand, reservoir quality as well as reservoir classification could be performed based on these data correlation. The Szolnok Formation is composed mainly of turbidity elastic deposits while siltstones are intercalated by sandstone beds and streaks of marls. In the present study, 213 core samples are obtained from the Szolnok Formation of the Great Hungarian plain, Hungary. Both horizontal and vertical permeability are measured. The Szolnok Formation has two main lithologic groups: 1. clean sandstone (141 samples) and 2. siltstone – marl (72 samples), it can easily differentiate between good, intermediate or even bad reservoirs. Acoustic laboratory measurements have been carried out for only 30 sandstone rock samples parallel to the bedding plane (horizontal). This paper aims to evaluate some petrophysical relationships. On the other hand, both Wyllie and Raymer models were applied for porosity estimation from seismic velocity. It is worthy to mention that reservoir diagnosis of the Szolnok Formation was our target as well. Both the porosity and permeability variation range characterizing the detected lithologic facies of the Szolnok Formation are useful for reservoir zonation. The relationship between helium and mercury porosity for whole studied samples and sandstone samples as well, are supported by a high correlation coefficient and allow its application for prediction of porosity while it reduces costs and time of laboratory measurements. The evaluation of different calculated equations for porosity from compressional wave velocity data of the Szolnok Formation are studied and the relationship between velocity and porosity displays a clear inverse trend. The comparison between laboratory porosity and sonic derived porosity shows that the values determined by Wyllie and Raymer equations are not applicable to predict it from velocity data.

© 2016 Egyptian Petroleum Research Institute. Production and hosting by Elsevier B.V. This is an open access article under the CC BY-NC-ND license (<http://creativecommons.org/licenses/by-nc-nd/4.0/>).

* Corresponding author. Fax: +20 22747433.

E-mail addresses: muktader76@yahoo.com, muktader76@sci.asu.edu.eg (A.M.A. El Sayed), heshamabuseda@yahoo.com, heshamabuseda@epri.sci.eg (H. Abuseda), nahlamuktader@hotmail.com (N.A. El Sayed).

¹ Fax: +20 22747433.

Peer review under responsibility of Egyptian Petroleum Research Institute.

<http://dx.doi.org/10.1016/j.ejpe.2016.03.004>

1110-0621 © 2016 Egyptian Petroleum Research Institute. Production and hosting by Elsevier B.V.

This is an open access article under the CC BY-NC-ND license (<http://creativecommons.org/licenses/by-nc-nd/4.0/>).

1. Introduction

The Szolnok Formation Fig. 1 of the Great Hungarian plain was our target of the present study. It is attributed to the Late Miocene age (Pannonian basin). The Great Hungarian plain lies in the south-eastern part of Hungary. The term Pannonian is mainly related to sedimentary facies which are ranged in age from the Miocene to the Pliocene and distributed within the Pannonian basin Fig. 2. The Pannonian basin is a large extension especially in the eastern part of Hungary. It is characterized by various sedimentary environments through time and space. While near shore, fluvial, alluvial and deltaic facies were the most predominant. The sedimentary sequence of the Pannonian basin in the Great Hungarian plain has been geological studied and stratigraphically classified by different authors e.g. [1,17]. The sedimentary sequences are developed in the Pannonian basin during the Miocene times. The prevailing environments of deposition seem to be unchanged through that long time. The lithologic associations formed in the Pannonian sub-basins are almost identical although these deposits are of younger age toward the southeastern part of the basin. The Szolnok Formation is mainly composed of sandstone beds intercalated with argillaceous marl, siltstones, coal seams, plant debris and fragments. Turbidity deposits characterizing the Szolnok Formation were created in a pro-delta sub-environments, while the northwestern direction of the delta system was prevailing. The Szolnok Formation is conformably underlined by calcareous marl of the Nagykorui Formation and overlain by the Algyo Formation.

The aim of the present study is to evaluate some petrophysical relationships and applying Wyllie and Raymer models for porosity estimation from acoustic velocity measured for some sandstone samples. It is worthy to mention that, the reservoir

diagnosis of the Szolnok Formation is the main target of the present study.

2. Samples and methods

Petrophysical laboratory investigations were carried out to determine petrophysical data such as porosity (measured by mercury and helium techniques), permeability (measured on horizontal and vertical samples), effective pore radius (pore throat distribution) and sonic wave velocity. The petrophysical methods that have been applied in our study are compiled in Table 1. We provide a detailed description of the petrophysical experiments and the resulting relations. We have started our study with a total of 213 cylindrical core samples obtained from the Szolnok Formation. The studied samples are classified into two groups one of them is clean sandstone (141 samples) and another group is siltstone and marl (72 samples) according to studies including petrographical and SEM analysis [15,18]. Before performing petrophysical measurements, samples were prepared as cylinders of 2.55 cm (1 inch) diameter and different lengths (from 3 to 5 cm) using a diamond drilling machine. At the same depth, we cut two samples one of them parallel to the bedding plane (horizontal), while the other one is perpendicular the bedding plane (vertical). Unfortunately, the sandstone and siltstone – marl samples are only weakly consolidated. Despite careful handling, some samples have been broken during the sample preparation, saturation, and the experiments. Therefore, the number of samples varies for the different experiments. Prior to the laboratory measurements of petrophysical properties, the original residual liquids are completely removed from the core samples using hot solvent extraction technique. [19,20]. The samples were considered to be clean of residual hydrocarbon when the extract

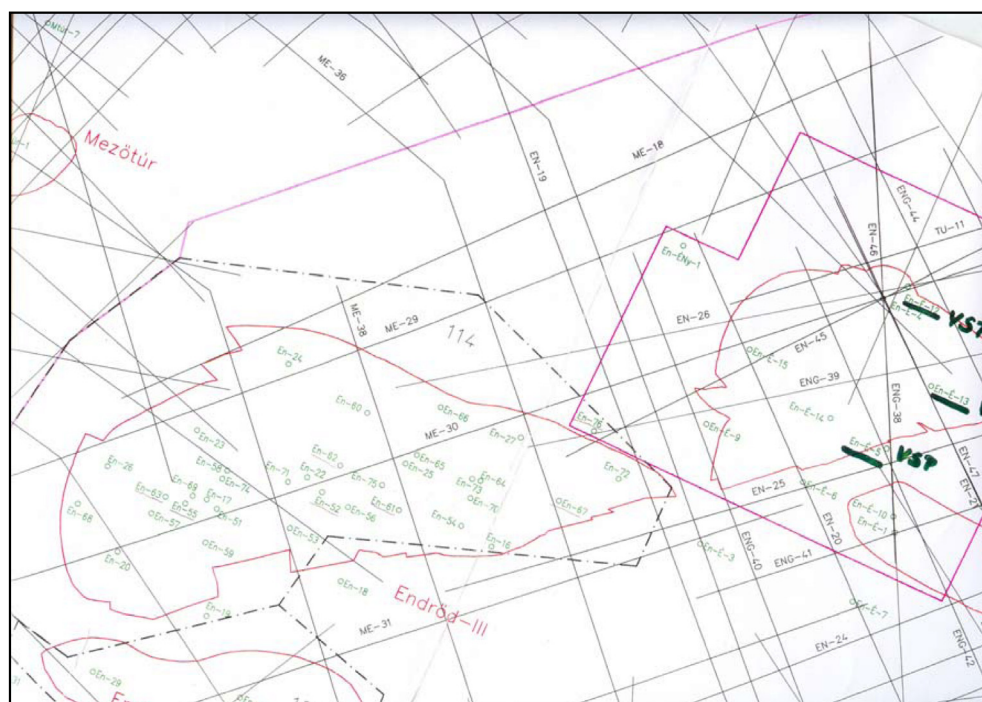


Figure 1 Location map of studied wells in the Endrod oil and gas field in Hungary.

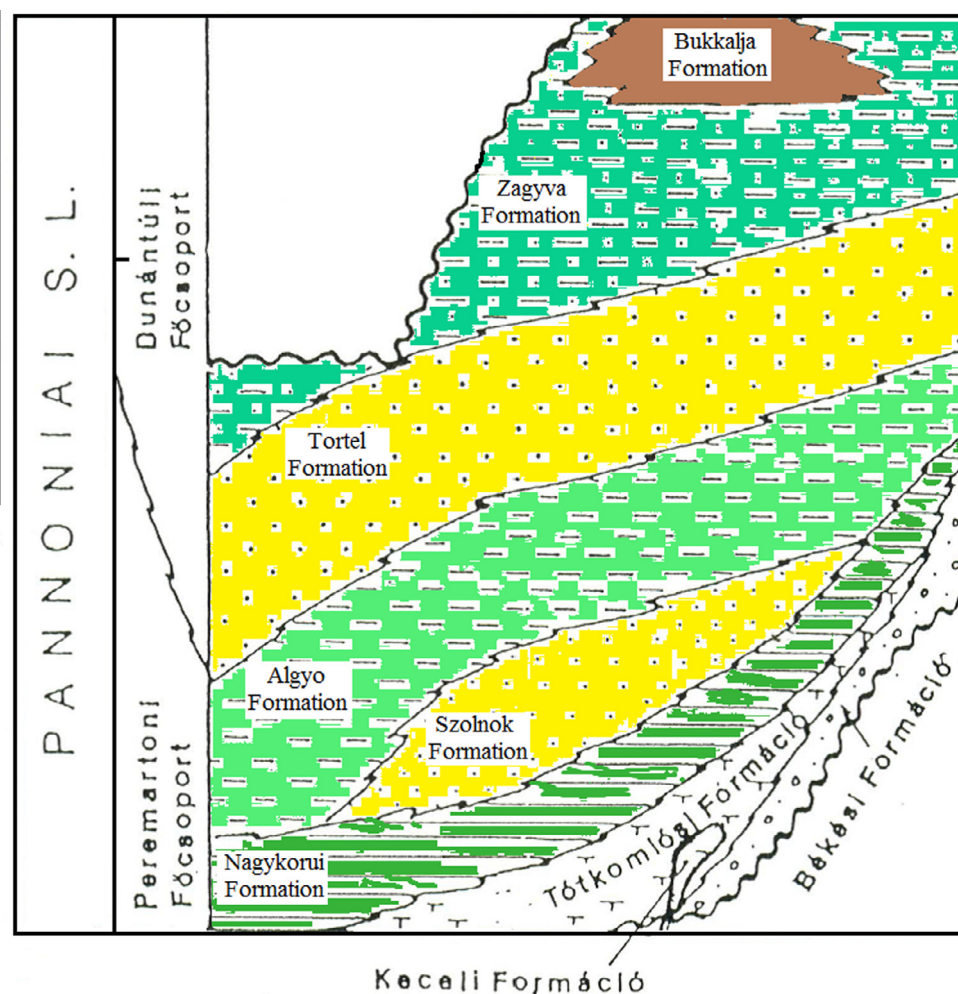


Figure 2 Stratigraphic classification of the Pannonian s.l. showing the Szolnok Formation.

Table 1 Petrophysical investigation techniques used for Szolnok Formation samples.

Measured petrophysical parameters					
Measured parameter	Parameter and symbol	Physical unit	Number of all samples	Number of sandstone samples	Number of siltstone – marl
Mercury porosity	Porosity: \varnothing_M	%	222	141	81
Helium porosity	Porosity: \varnothing_H	%	217	141	76
Effective pore radius	$P_{1.87}$	μm	168	131	37
Horizontal permeability	Permeability: K_H	mD	211	141	70
Vertical permeability	Permeability: K_V	mD	185	133	52
Compressional wave velocity	P-wave velocity: V_p	m/s	30	30	–
Shear wave velocity	S-wave velocity: V_S	m/s	30	30	–

(in direct contact with samples) is colorless and the core plugs did not show any fluorescence when viewed under ultra violet light [19]. Samples are considered at constant weight, when taken before and after a subsequent four hour drying period, are repeatable to ± 0.01 g. After the constant weight had been achieved all the samples were allowed to cool to room temperature in moisture free desiccators.

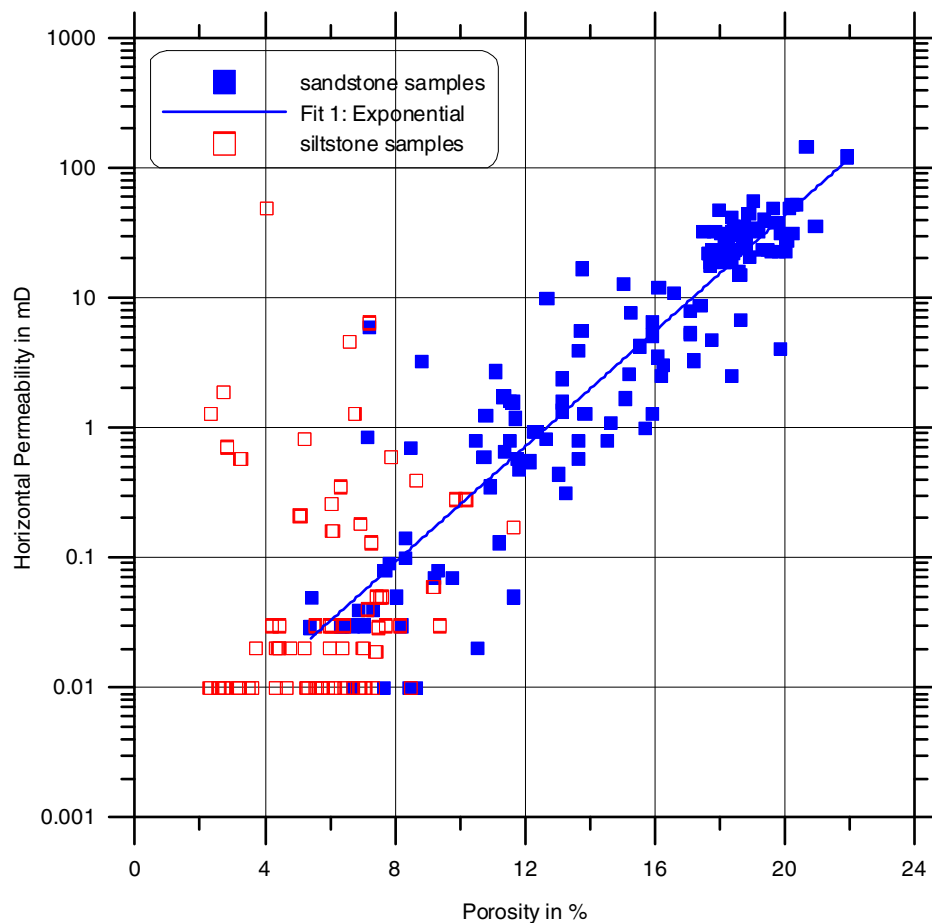
3. Experimental work

3.1. Porosity

The porosity of the studied samples has been determined by the helium porosimeter method. While permeability was measured using Hassler type core holder while, the pore throat

Table 2 Compilation of minimum, maximum, average values and standard deviations of measured petrophysical parameters for Szolnok Formation.

Compilation of petrophysical parameters												
Parameters	All samples				Sandstone samples				Siltstone – marl			
	Min.	Max.	Mean	Std. dev.	Min.	Max.	Mean	Std. dev.	Min.	Max.	Mean	Std. dev.
Porosity: ϕ_M , %	1.26	20.67	3.90	4.08	1.88	20.67	12.26	4.21	1.26	9.16	4.31	2.01
Porosity: ϕ_H , %	2.31	21.91	11.72	5.74	5.39	21.91	14.92	4.37	2.31	11.65	5.78	2.05
$P_{1.87}$, μm	0.01	16.48	3.90	4.08	0.01	16.48	4.98	4.00	0.01	0.19	0.06	0.05
Permeability: K_H , md	0.01	145.07	10.43	18.39	0.01	145.07	15.12	20.59	0.01	48.36	1.00	5.82
Permeability: K_V , md	0.01	84.87	6.56	11.56	0.01	84.87	9.08	12.78	0.01	3.35	0.11	0.47
P-wave velocity: V_p , m/s	–	–	–	–	1170	3330	2283	526	–	–	–	–
S-wave velocity: V_s , m/s	–	–	–	–	900	2360	1533	403	–	–	–	–

**Figure 3** Porosity versus horizontal permeability for sandstone and siltstone – marl samples of the Szolnok Formation.

size distribution is determined using mercury injection technique (MICP). The prepared clean (hydrocarbon free) sample is placed in a metal chamber of Carlo Erba porosimeter (model 2000) and then evacuated. Mercury is forced into the evacuated core sample at low pressure starting with 1.0 kg/sq.cm, which is maintained until no more mercury enters the sample. The volume of mercury entering the sample at this pressure level is recorded by the pressure measuring circuit of the used porosimeter. The process is repeated through a range of pressure (1.0–2000.0 kg/sq.cm) while the recorded volume of mercury injected with each pressure increment step is used

for calculating directly the percentages of total pore spaces which can be saturated. The fraction of the one volume accounted by all pore sizes between 75,000 Å and 37 Å is calculated according to the following equation;

$$V_p = (H_{pmax} - H_{pr})/H_{pmax} \quad (1)$$

where

H_{pmax} = corrected value of mercury level displacement in mm at maximum pressure,

H_{pr} = corrected value of mercury level displacement in mm at pressure step recorded.

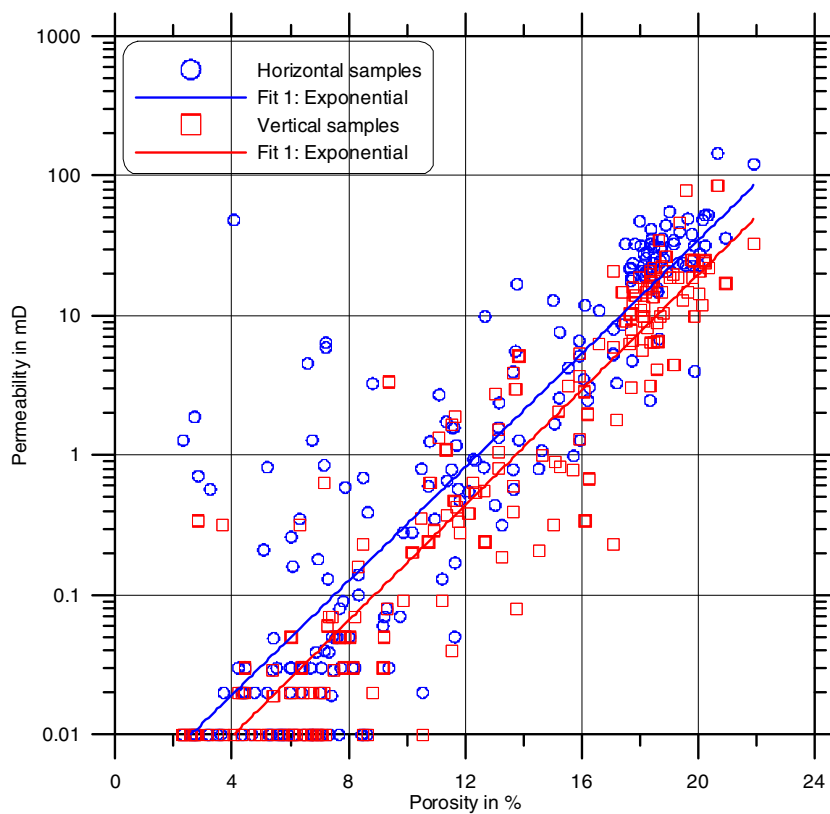


Figure 4 Porosity versus horizontal and vertical permeability for all samples of the Szolnok Formation.

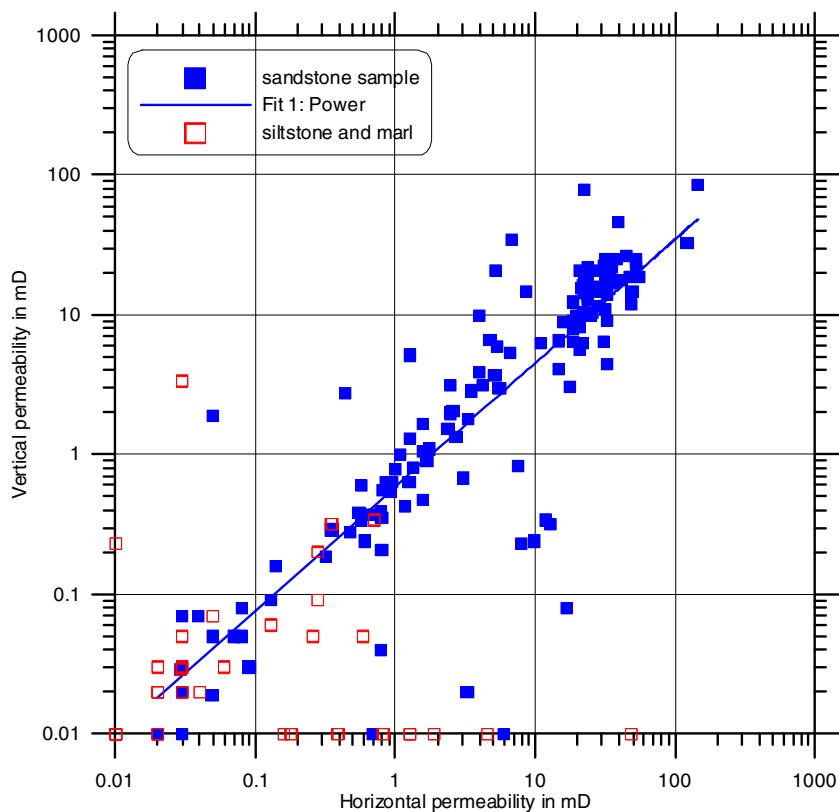


Figure 5 Horizontal permeability versus vertical permeability for sandstones and siltstone – marl samples of the Szolnok Formation.

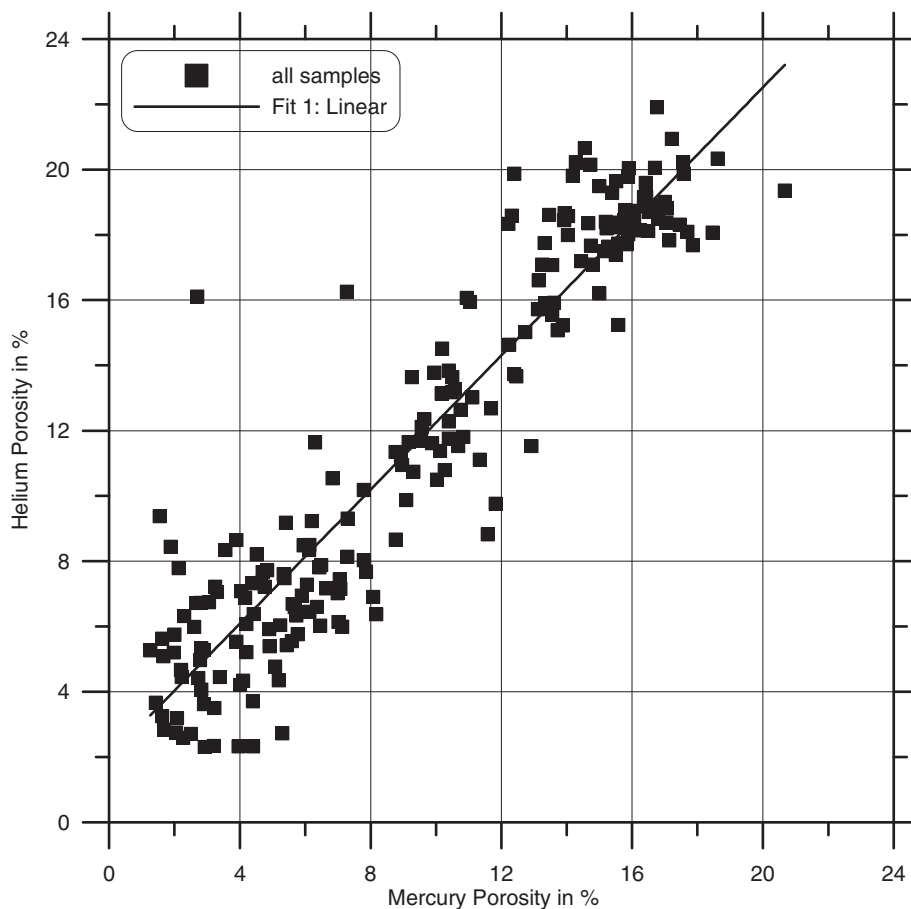


Figure 6 Mercury porosity versus helium porosity for all studied samples of the Szolnok Formation.

The sample mercury porosity, in the present work, is determined according to equation

$$\emptyset = (a \cdot H_{pmax} \cdot Q) / A \cdot L \quad (2)$$

where

\emptyset = effective porosity, fraction,

a = the instrument dilatometer cross sectional area sq.mm,

Q = Sample weight in g., while it is referred to one gram of sample,

A = core sample cross sectional area, sq.mm,

L = core sample length.

On the other hand, the sample helium porosity is determined by use of both universal mercury porosimeter for bulk volume (V_b) determination and the helium porosimeter with matrix cup core holder for grain volume (V_g) estimation. Hence, porosity is calculated as

$$\emptyset = 1.0 - (V_g / V_b) \quad (3)$$

3.2. Permeability

The permeability (non-scalar parameter) of a rock is affected by many geological primary structures like lamination [21]. A pore network is made up of larger spaces that are referred to as pores, which are connected by small spaces referred to as pore throats. In other words, the volume of pore space is

reflected by the measured porosity, while the size of pore throats is reflected by the measured permeability of a rock. The geometric relationship between pore spaces and pore throats controls the relationship between porosity and permeability. The relationship between porosity and permeability has been studied by many authors, e.g. [22,29].

The permeability (K) of all samples was measured by using Hassler type core holder in which sample was subjected to dry Nitrogen gas with a pressure of 1378.9 kPa. The gas permeability is calculated as;

$$K = \{(C \cdot Q \cdot h_w \cdot L) / 200 \cdot V_b\} \quad (4)$$

where

K = permeability μm ,

C = value of mercury height mm,

Q = orifice value,

h_w = orifice manometer reading mm,

L = sample length cm,

V_b = sample bulk volume cubic cm.

3.3. Effective pore radius

Pore throat size distribution is outlined using mercury injection technique by using porometer –2000 with a maximum pressure 30,000 psi. The pore radius in sandstone reservoirs usually ranged from 0.0075 μm up to 7.5 μm or more. The effective pore radius for hydrocarbon production is identified

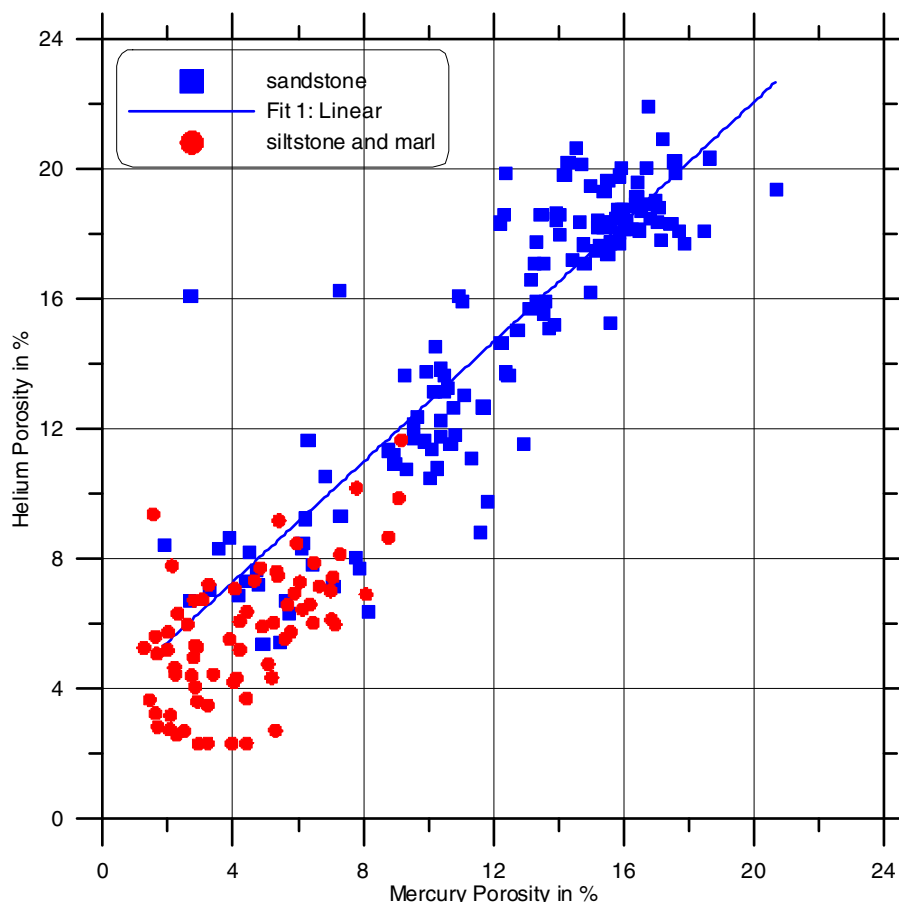


Figure 7 Mercury porosity versus helium porosity for sandstone and siltstone – marl samples of the Szolnok Formation.

as $0.5 \mu\text{m}$ [30] while the size equal to $1.87 \mu\text{m}$ is suggested by [16] and it is called P1.87.

3.4. Sonic wave velocity

Seismic body waves exist in two types, as compressional wave and shear wave with the velocities V_p and V_s . The velocity of propagation in an isotropic elastic medium is a function of Lamé's parameters and rock density. These parameters may be expressed in terms of bulk modulus, shear modulus and Poisson's ratio. In the present work, compressional and shear velocities were measured at room temperature and ambient pressure on cylindrical samples using a two channel Sonic Viewer (OYO – 170). The instrument performs fast sampling and digital recording. Stacking in 16 bit memory improves the signal to noise ratio and widens its applicability to weak signals. The P-wave and S-wave velocities have been measured at ultrasonic frequencies of 63 kHz and 33 kHz, respectively.

4. Petrophysical models

4.1. Sonic wave velocity and porosity

The fundamental equation formulated by [31] relates the velocities of the sample (v_p) to the porosity (\emptyset), the velocity of the solid material v_s , and the velocity of the pore v_A :

$$\frac{1}{v_p} = \frac{(1 - \emptyset)}{v_s} + \frac{\emptyset}{v_A} \quad (5)$$

If all the velocity values are known, Eq. (5) can be transformed to determine an acoustic porosity \emptyset_w :

$$\emptyset_w = \frac{v_A}{v_p} \left(\frac{v_s - v_p}{v_s - v_A} \right). \quad (6)$$

The acoustic porosity has to be compared to the measured porosity to verify the applicability of the Wyllie equation (Eq. (5)).

Another empirical equation was proposed by [32] as an alternative to the time average equation for interpretation of acoustic logs

$$v_p = (1 - \emptyset)^2 \cdot v_s + \emptyset \cdot v_A \quad (7)$$

An acoustic porosity \emptyset_R can be determined from the solution of this quadratic equation:

$$\emptyset_R = \frac{1}{2v_s} \left\{ (2v_s - v_A) - \sqrt{v_A^2 + 4v_s(v - v_A)} \right\} \quad (8)$$

Another empirical model is compared to the porosity estimation from compressional wave velocity for Egyptian sandstone and carbonate samples [33,34].

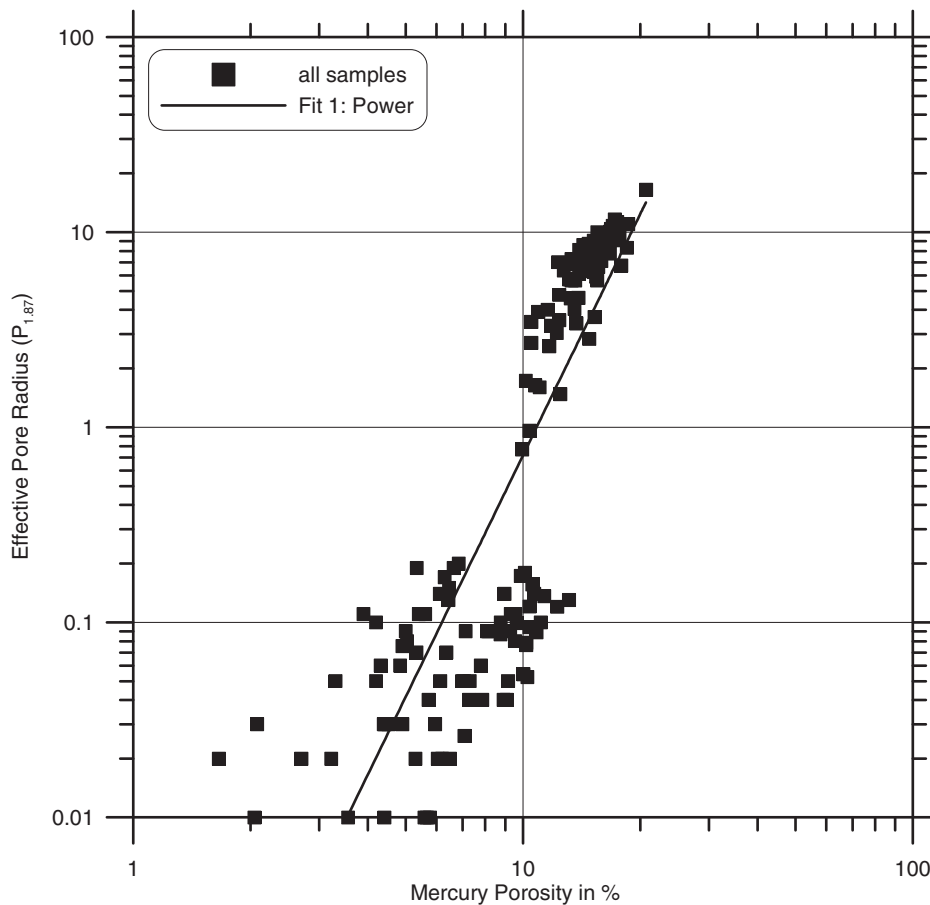


Figure 8 Mercury porosity versus the calculated effective pore space radius for all samples of the Szolnok Formation.

5. Results

The minimum, maximum, average values and standard deviations of all measured parameters of the studied samples of the Szolnok Formation are compiled in Table 2. The Mercury Porosity values of the studied samples vary from 1.26% to 20.67% with a mean value of 3.90%. But helium porosity has higher values than mercury and vary from 2.31% to 21.91% with a mean value of 11.72%. The database shows a considerable variation in both horizontal permeability (from 0.01 mD to 145.07 mD), and vertical permeability (from 0.01 mD to 84.87 mD). The measured compressional wave velocity varies between 1170 m/s and 3330 m/s with a mean value of 2283 m/s, while shear wave velocity varies from 900 m/s to 2360 m/s with a mean value of 1533 m/s. The following part is devoted to discuss the performed cross plots concerning with reservoir diagnostic features.

6. Petrophysical relationships

6.1. Porosity and permeability

The relation between porosity and horizontal permeability that is displayed in Fig. 3 indicates the expected trend for sandstone

samples and is characterized by coefficients of determinations ($R^2 = 0.83$), while for siltstone are shown data points that are highly scattered, have mainly cloud sample point shape and very weak coefficients of determinations ($R^2 = 0.03$), indicating that permeability does not depend on the sample porosity in the case of marl-siltstone and we noted constant values for permeability and change in porosity values in most marl-siltstone samples. The calculated equation controlling this relation is:

For sandstone samples:

$$K_H = [10]^{(0.22\phi - 2.83)} \quad (9)$$

where

ϕ : porosity in %,

K_H : horizontal permeability in mD.

The porosity – permeability cross plot for horizontal and vertical samples is shown in Fig. 4. The resulting correlations shown in these figure are characterized by reliable coefficients of correlation for both horizontal and vertical samples ($R^2 = 0.77$ and $R^2 = 0.87$), respectively, and we note that the horizontal samples showing slightly higher permeability than the vertical one. The porosity – permeability relationship for horizontal and vertical samples is controlled by the following equations:

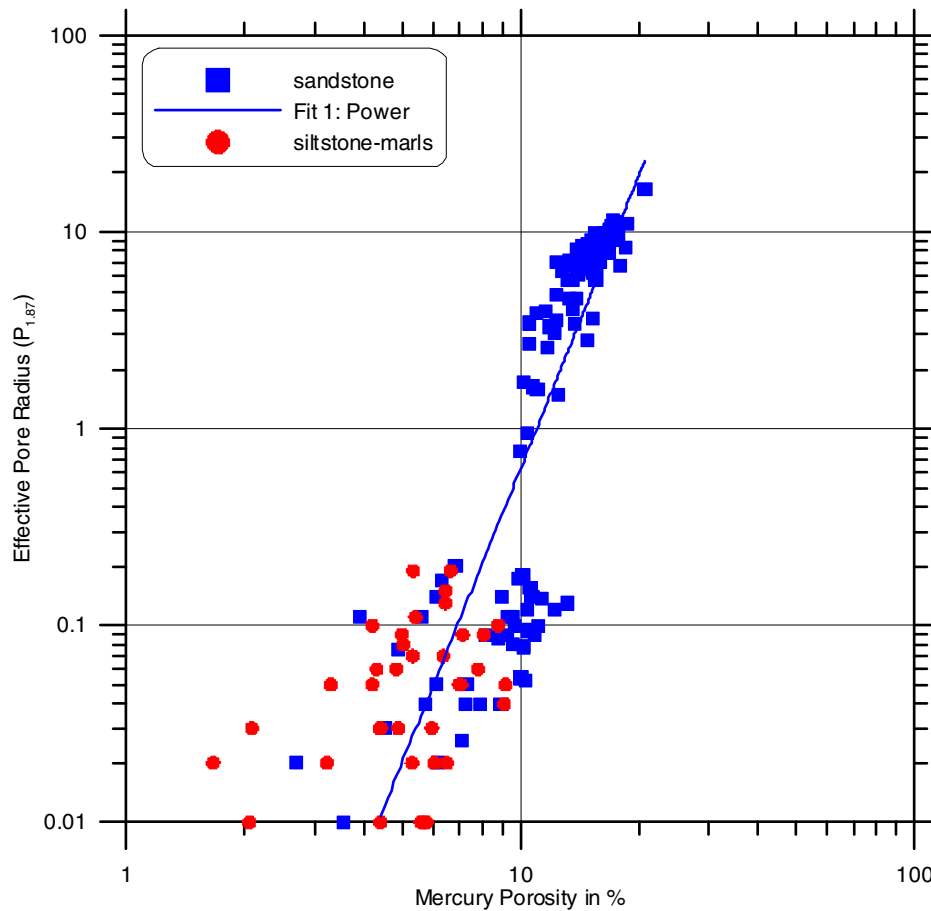


Figure 9 Mercury porosity versus effective pore space radius for sandstone and siltstone – marl samples of the Szolnok Formation.

For horizontal samples:

$$k = [10]^{(0.20\emptyset - 2.53)}, \quad (10)$$

For vertical samples:

$$k = [10]^{(0.21\emptyset - 2.84)}. \quad (11)$$

where

\emptyset : porosity in %,

k : permeability in mD.

The relationship between horizontal permeability and vertical permeability of the Szolnok Formation gives clear diagnostic features for reservoir heterogeneity in case of siltstone – marl as shown in Fig. 5, and characterized by reliable coefficients of correlation ($R^2 = 0.72$) for sandstone samples and controlled by the following equation:

$$\log K_v = 0.89 \log K_H - 0.53 \quad (12)$$

where

K_v : vertical permeability in mD,

K_H : horizontal permeability in mD.

while for siltstone – marl the data points are highly scattered and very weak coefficient of correlation ($R^2 = 0.01$) as shown in Fig. 5.

6.2. Mercury versus helium porosity

The relationship between helium porosity and mercury porosity is shown in Fig. 6 for all samples, while, Fig 7 elucidates sandstone and siltstone – marl facies. The data points in these figures follow the positive trend between mercury porosity and helium porosity and are characterized by close coefficients of correlation ($R^2 = 0.87$ and 0.79) for all and sandstone samples respectively and weak coefficients of correlation ($R^2 = 0.36$) for siltstone – marl while, this relationship is controlled by the following equations:

For all samples:

$$\emptyset_H = 1.03\emptyset_M + 1.98, \quad (13)$$

For sandstone samples:

$$\emptyset_H = 0.92\emptyset_M + 3.60, \quad (14)$$

where

\emptyset_H : helium porosity in %,

\emptyset_M : mercury porosity in %.

The equations for all and sandstones are supported by a high correlation coefficient allowing its application for prediction mercury porosity from the other. It is worthy to mention that both the defined sandstone and siltstone – marl discrimi-

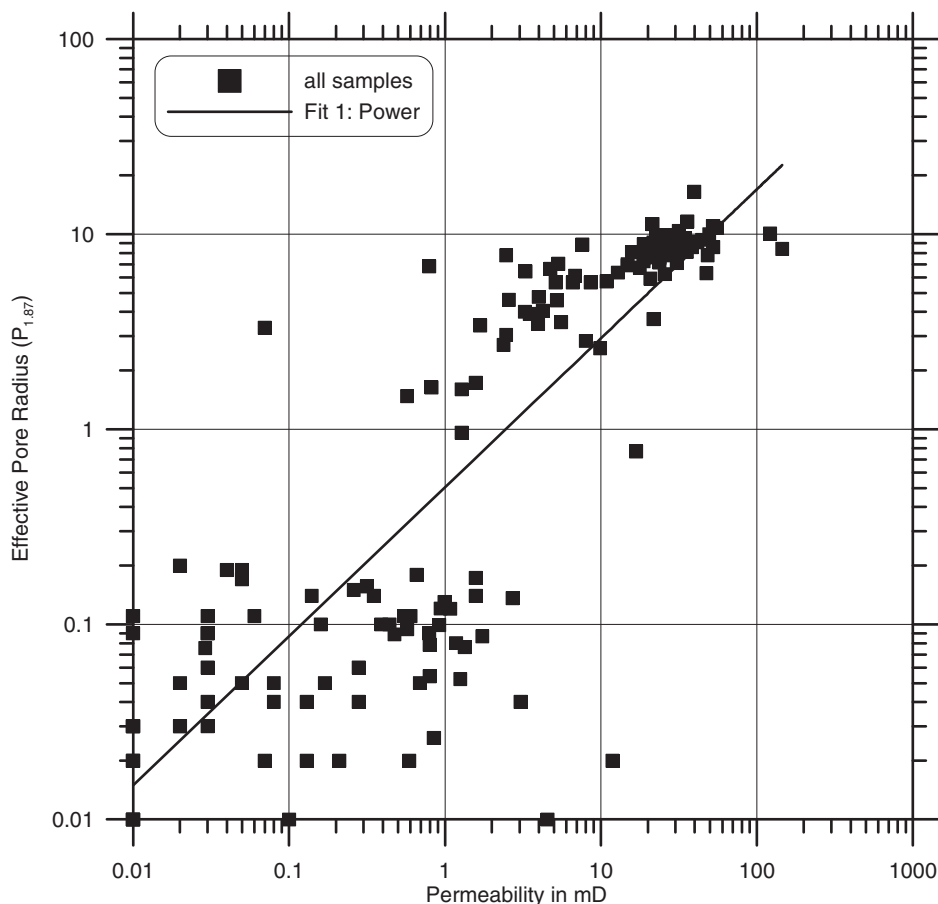


Figure 10 Permeability versus effective pore space radius for all samples of the Szolnok Formation.

nant areas as shown in Fig. 7 could be beneficial during the lithofacies studies of Szolnok Formation.

6.3. Effective pore space radius versus mercury porosity and permeability

The effective pore space radius, in the present study, is defined as the pore volume corresponding to a pore radius of 1.87 μm in size [16]. The relationships between effective pore radius and mercury porosity, permeability for all samples, sandstone and siltstone – marl are slightly useful for facies discrimination, however they exhibit linear trends in the case of clean sandstone samples. It is clear that effective pore space radius has little or no positive contribution to increase porosity and permeability in the case of siltstone – marl facies of the Szolnok Formation. By using these relations one can determine the effective pore radius which is difficult in measurements and expensive too from the routine porosity data of the Szolnok Formation.

The data points in Figs. 8 and 9 follow the positive trend between mercury porosity and effective pore radius and are characterized by reliable coefficients of correlation ($R^2 = 0.75$ and 0.73) for all and sandstone samples respectively and very weak coefficients of correlation ($R^2 = 0.14$) for siltstone – marl. This relationship is controlled by the equations:

For all samples:

$$P_{1.87} = [10]^{(-4.26)} * [\varnothing_M]^{(4.11)}. \quad (15)$$

For sandstone samples:

$$P_{1.87} = [10]^{(-5.17)} * [\varnothing_M]^{(4.97)} \quad (16)$$

where

$P_{1.87}$: effective pore radius, μm ,

\varnothing_M : mercury porosity in %.

The data points in Figs. 10 and 11 follow the positive trend between permeability and effective pore space radius and are characterized by reliable coefficients of correlation ($R^2 = 0.73$ and 0.67) for all and sandstone samples respectively and very weak coefficients of correlation ($R^2 = 0.02$) for siltstone – marl and this relationship is controlled by equations:

For all samples:

$$P_{1.87} = [10]^{(-0.30)} * [K_H]^{(0.76)}, \quad (17)$$

For sandstone samples:

$$P_{1.87} = [10]^{(-0.29)} * [K_H]^{(0.79)}. \quad (18)$$

where

$P_{1.87}$: effective pore radius, μm ,

K_H : horizontal permeability in mD.

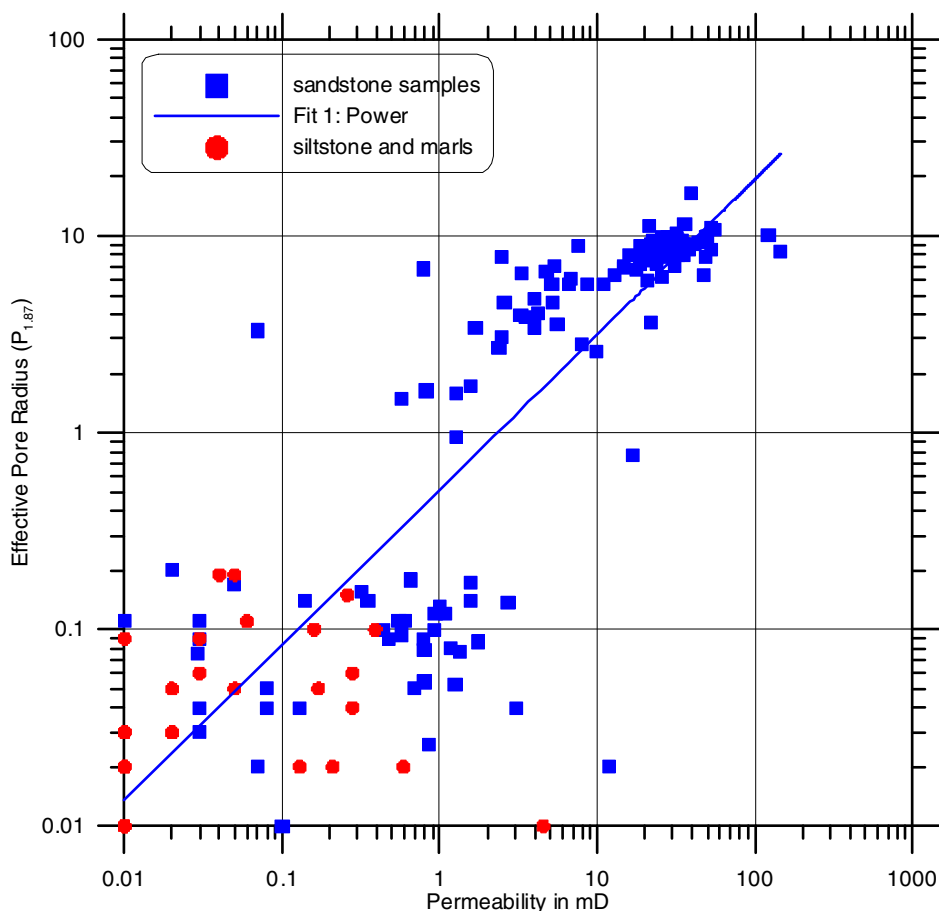


Figure 11 Permeability versus effective pore space radius for sandstone and siltstone – marl samples of the Szolnok Formation.

6.4. P-wave velocity – porosity

The P-wave velocity – porosity relationship for the studied samples is shown in (Fig. 12). The relationship is characterized by a fair coefficient of correlation ($R^2 = 0.38$). The P-wave velocity – porosity shows a reverse relation. P-wave velocity decreases with increasing porosity. The relationship is controlled by the equation:

$$V_p = 3436.54 - 5882.67\phi \quad (19)$$

where

ϕ : porosity in fraction,

V_p : compressional wave velocity m/s.

6.5. S-wave velocity – porosity relationship

The S-wave velocity – porosity relationship for the studied samples is shown in (Fig. 13). The relationship is characterized by a fair coefficient of correlation ($R^2 = 0.50$). The S-wave velocity – porosity shows a reverse relation. S-wave velocity decreases with increasing porosity. The relationship is controlled by the equation:

$$V_s = 2671.84 - 6317.59\phi \quad (20)$$

where

ϕ : porosity in fraction,

V_s : shear wave velocity m/s.

6.6. Velocity – porosity relations

Eq. (6) was used to determine the acoustic porosities ϕ_w of the sandstone samples. The velocity of quartz $v_{quartz} = 6040$ m/s is used as velocity of the solid material v_s of a sandstone. For the dry samples, the pore space is filled with air and the velocity of air is $v_A = v_{air} = 330$ m/s. The comparison between the measured porosity and the acoustic porosity calculated from Wyllie equation using Eq. (6) is shown in Fig. 14. It should be noted that the variation in the measured porosity is higher than in the predicted by Wyllie equation. Fig. 15 displays the comparison between the measured porosity and the acoustic porosities ϕ_R calculated from Eq. (8), results generally in higher predicted porosity. It should be noted that the variation in the measured porosity is lower than that predicted by Raymer's equation.

7. Porosity prediction

We compare models of porosity prediction that are based on acoustic velocities, which have been determined for the sand-

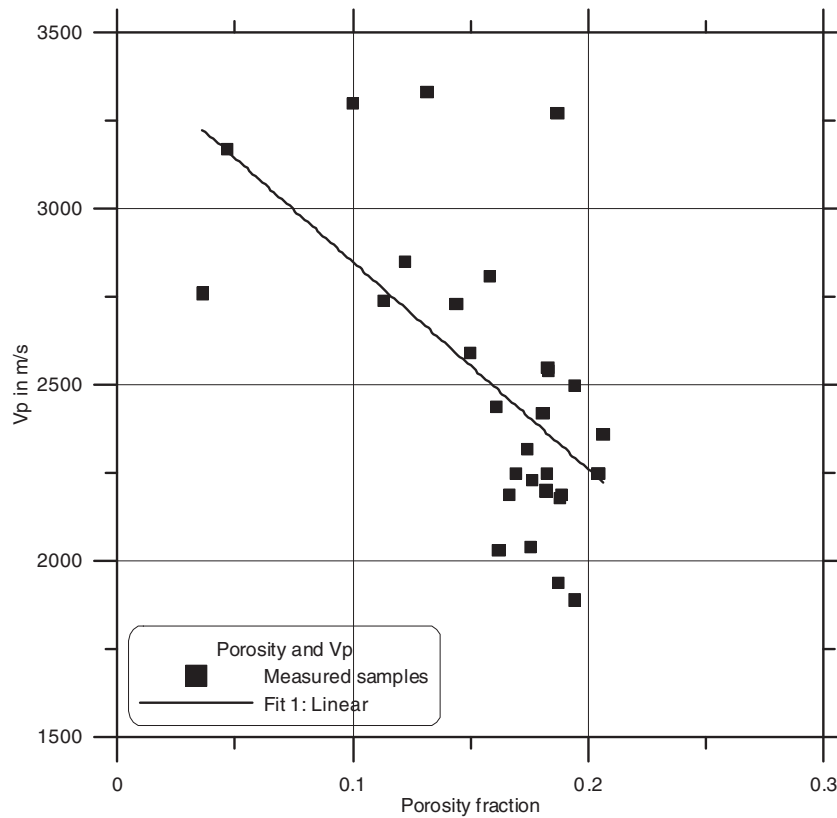


Figure 12 P-wave velocity versus porosity for all samples of the Szolnok Formation.

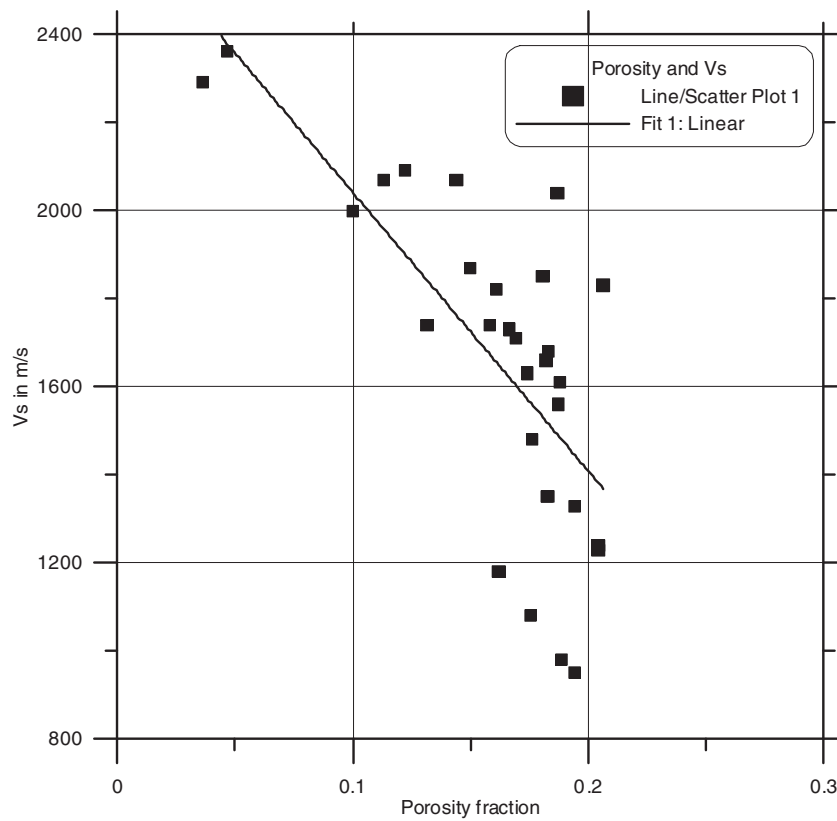


Figure 13 S-wave velocity versus porosity for all samples of the Szolnok Formation.

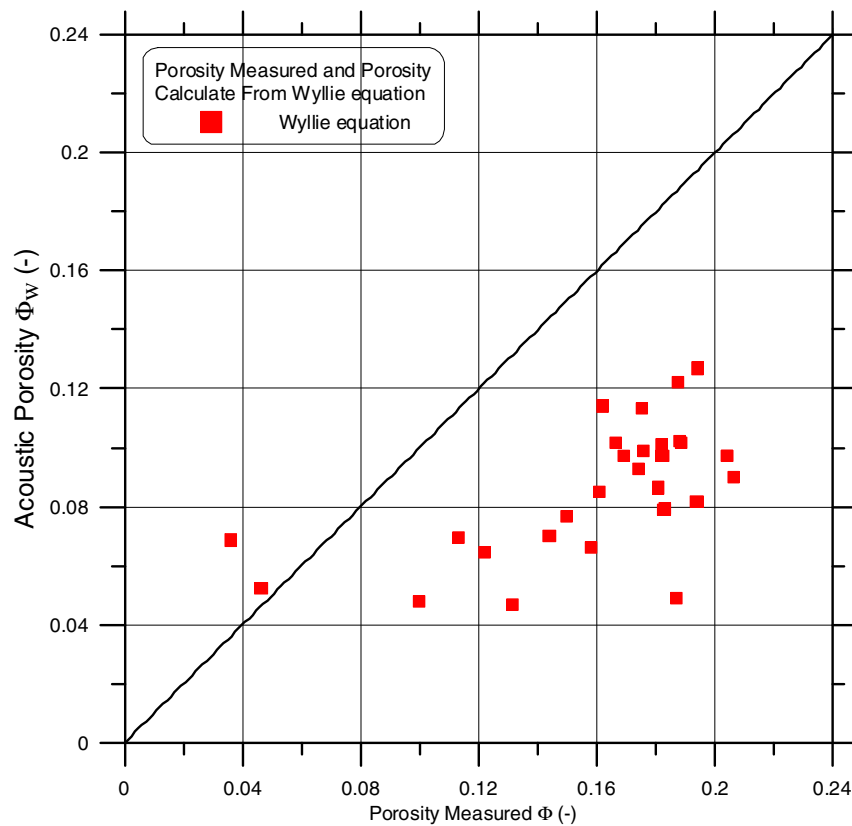


Figure 14 Comparison between measured porosity and acoustic porosity calculated using Wyllie-equation for Szolnok Formation.

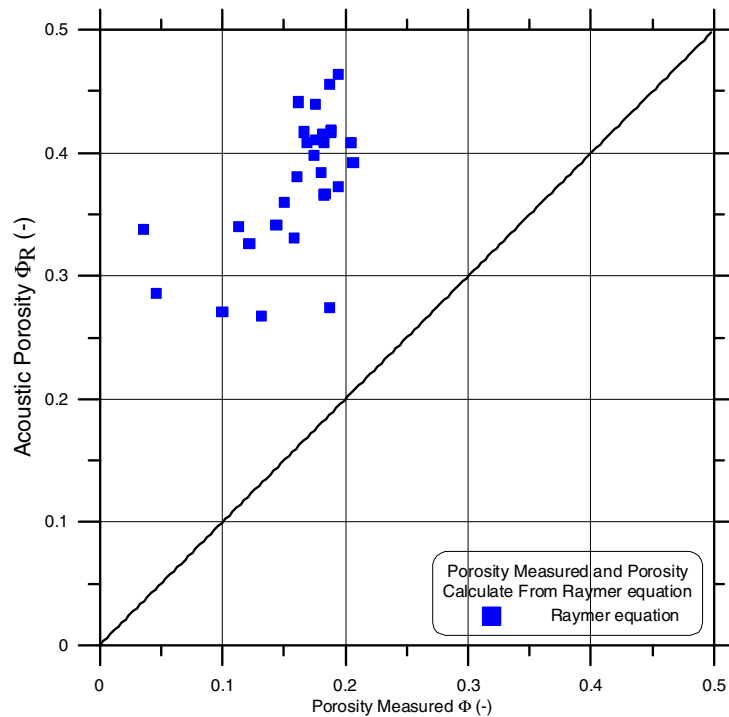


Figure 15 Comparison between measured porosity and acoustic porosity calculated using Raymer-equation for Szolnok Formation.

Table 3 Root mean square (*rms*) division between measured porosity and acoustic porosity resulting from Wyllie and Raymer equation.

Parameters	<i>rms</i>	\bar{d}
$\varnothing_w = \frac{v_A}{v_p} \left(\frac{v_s - v_p}{v_s - v_A} \right)$	0.30	0.29
$\varnothing_R = \frac{1}{2v_s} \left\{ (2v_s - v_A) - \sqrt{v_A^2 + 4v_s(v - v_A)} \right\}$	0.41	0.39

stone samples of our study. To evaluate the predictive power of the models, the root mean square (*rms*) error quantifies the deviation between the measured and acoustic porosities (\varnothing^*) which is determined as follows:

$$rms = \sqrt{\frac{1}{n} \sum_{i=1}^n (\log_{10} \varnothing - \log_{10} \varnothing_i^*)^2} \quad (21)$$

with *n* being the number of considered samples. In addition to the *rms*, the average deviation between calculated and measured porosity is given by

$$\bar{d} = \frac{1}{n} \sum_{i=1}^n |\log_{10} \varnothing - \log_{10} \varnothing_i^*| \quad (22)$$

are used to evaluate the quality of porosity prediction. Table 3 compiles the *rms* resulting from all investigated equations used for the sandstone samples.

8. Conclusions

The studied petrophysical data obtained for the Szolnok Formation have been treated as one population for all samples (213 samples) that is divided into two groups, one of them is clean sandstone (141 samples) and another group is siltstone and marl (72 samples). We can easily differentiate between good and intermediate or even bad reservoirs among the Szolnok Formation, while, each lithologic facies has a characteristic trend. The prediction of porosity and/or permeability from the other reservoir parameter is of great significance for Szolnok reservoir evaluation.

Both the porosity and permeability variation range characterizing each detected lithologic facies of the Szolnok Formation is useful for reservoir synergy and zonation. The relationship between helium and mercury porosity for all as well as sandstone samples are supported by a high correlation coefficient and allow its application for prediction of one parameter from the other, while it reduces costs and time of laboratory measurements. Some pore volume sizes especially effective pore radius (1.87 μm) could be predicted from either measured permeability or porosity. The relationships between effective pore space radius and porosity/permeability are useful for facies discrimination, however they exhibit linear trends

in the case of clean sandstone samples. It is clear that effective pore space radius has little or no positive contribution for increased porosity and permeability in the case of siltstone – marl facies of the Szolnok Formation. By using these relations one can determine the effective pore space radius which is difficult in measurements and expensive too from the routine porosity data of the Szolnok Formation. The evaluations of different existing equations for porosity from compressional wave velocity data of the Szolnok Formation are studied and the relationship between compressional wave velocity and porosity displays a clear inverse trend. The comparison between measured and sonic derived porosity shows that the values determined by Wyllie equation are not applicable to predict porosity from P-wave velocity data. Raymer equation results generally in higher predicted porosity.

Acknowledgments

Authors gratefully acknowledged the financial support of the Hungarian MOL Rt during the laboratory work and in data and sample collection and preparation.

References

- [1] M. Szeles, Foldt. Kozlony 92 (1962) 53–60.
- [15] A.M.A. El Sayed, B. Kiss, Geophys. Trans. 41 (1–2) (1997) 37–63.
- [16] A.M.A. El Sayed, I. Berczi, B. Kiss, in: 5th meeting environmental and engineering geophysics (EEGS-ES), Budapest, Hungary, 1999.
- [17] A.M.A. El Sayed, A. Abass, in: 11th International Conference on Mining, Petroleum and Metallurgical Engineering, 2009, pp. 789–801.
- [18] A.M.A. El Sayed, A. Abass, in: 11th International Conference on Mining, Petroleum and Metallurgical Engineering, Sharm El-Sheikh, 15–19 March, 2009, pp. 789–801.
- [19] API specifications, in: API recommended practice for core analysis procedure, RP 40, first ed., 1960, p. 49. August.
- [20] D.K. Keelan, Core analysis Techniques and Applications, SPE 4160, 1972.
- [21] N.A. El Sayed, A.M.A. El Sayed, Proc. Earth Planet. Sci. 15 (2015) 518–525.
- [22] P.C. Carman, Trans. Inst. Chem. Eng. 15 (1937) 150–166.
- [29] D. Tiab, E.C. Donaldson, Petrophysics: Theory and Practice of Measuring Reservoir Rock and Fluid Transport Properties, Elsevier, 2004.
- [30] E.D. Pittman, AAPG Bull. 76 (1992) 191–198.
- [31] M.R.J. Wyllie, A.R. Gregory, G.H.F. Gradnet, Geophysics 21 (1956) 41–70.
- [32] L.L. Raymer, E.R. Hunt, J.S. Gardner, in: Presented at the Soc. Prof. Well Log Anal. 21st. Ann. Mtg., Paper P, 1980.
- [33] M.A. Kassab, Andreas Weller, J. Petrol. Sci. Eng. 78 (2011) 310–315.
- [34] M.A. Kassab, Andreas Weller, J. Earth Sci. Eng. 3 (2013) 314–321.